Equivalent Circuit Model for Metamaterial-Based Electromagnetic Band-Gap Isolator

Young Jun Song, *Student Member, IEEE*, and Kamal Sarabandi, *Fellow, IEEE*

***Abstract*—This letter describes the performance characteristics of single-layer 1-D periodic resonant structures embedded in a metal-backed substrate. Such structures are known to behave as an electromagnetic band-gap (EBG) layer that can suppress the dominant substrate mode. For short distances in thin substrates, it is shown that the dominant $\mathrm{TM}_0^{\mathrm{odd}}$ with a zero cutoff frequency can be approximated by a TEM wave inside and in the vicinity of the thin substrate. The propagation of this TEM wave is then modeled by an equivalent transmission-line model. The effect of the resonant EBG structure on the wave propagation in the equivalent transmission-line model is taken into consideration by modeling the EBG structure in terms of an equivalent LC circuit and establishing the proper electric and magnetic mutual couplings between the LC circuit and the transmission-line model. The performance of the equivalent circuit model is compared to the full-wave simulation of the actual structure, and a very good agreement is shown.**

***Index Terms*—Electromagnetic band-gap (EBG) materials, electromagnetic shielding, interference suppression, mutual coupling.**

I. Introduction

IN RECENT years, electromagnetic band-gap (EBG) structures have been widely utilized in applications where mutual coupling between two or more closely spaced antennas is to be suppressed. Such applications include reduction of the mutual coupling among antenna elements of planar microstrip arrays [1], reduction of crosstalk in miniaturized elements of compact arrays [2], and more recently improved isolation among antennas of multiple-input–multiple-output (MIMO) communication systems [3], [4]. In practice, EBG materials are made of subwavelength magneto-dielectric structures with particular resonant characteristics that can inhibit wave propagation near their resonance [5], [6]. In such scenarios, usually the effective permeability of the equivalent medium becomes negative. Similar behavior has also been demonstrated for designing antennas over high impedance surfaces [7] and reactive impedance surfaces [8].

Manuscript received September 14, 2012; accepted November 07, 2012. Date of publication November 15, 2012; date of current version December 04, 2012. This work was supported by the U.S. Army Research Laboratory under Contract W911NF and prepared through collaborative participation in the Microelectronics Center of Micro Autonomous Systems and Technology (MAST) Collaborative Technology Alliance (CTA).

The authors are with the Radiation Laboratory, Department of Electrical Engineering and Computer Science, The University of Michigan at Ann Arbor, Ann Arbor, MI 48109-2122 USA (e-mail: yjsong@umich.edu; saraband@eecs.umich.edu).

Color versions of one or more of the figures in this letter are available online at http://ieeexplore.ieee.org.

Digital Object Identifier 10.1109/LAWP.2012.2227664

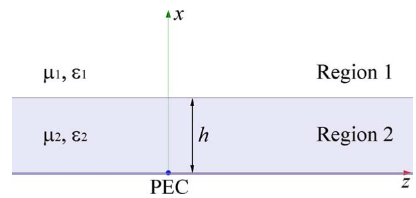

Fig. 1. Geometry of dielectric coated conductor.

Due to the assumption of periodicity of EBG structures, the design procedure often relies on calculation of dispersion diagram for a unit cell. Such analyses are based on Floquet theorem and do not account for the truncation effects that are encountered in practical situations. The numerical simulation of finite structures composed of numerous unit cells has features with dimensions much smaller than a wavelength. Thus, this requires significant computational resources, and the computational errors for such resonant structures usually exceed the required fidelity for an accurate design. One such problem is encountered in the design of an EBG structure intended for creating high isolation between two miniaturized antennas with subwavelength separation implemented in a thin substrate [9].

In order to address these difficulties, a new equivalent circuit model for such EBG structures is presented in this letter. A typical EBG structure, composed of two short-circuited vertical pins connected by a series capacitor, is considered here to understand the physical interactions between the substrate mode and the EBG isolator. Based on a previous design [9], the lateral dimension of the interdigital capacitor is decreased, and the height of the unit cell is increased to minimize the parasitic effects from the ground plane. The proposed equivalent circuit model employs a conventional transmission-line model embedding a magnetically coupled parallel LC resonant circuit. The circuit simulation and full-wave simulation responses are compared to show the validity of the proposed circuit model. It is shown that the proposed circuit model can correctly predict the reflection zero and the notch responses obtained from the full-wave simulation response.

II. Investigation of Substrate Modes

In most practical applications, RF communication circuits are built on dielectric substrates for system integration and miniaturization. A single-layer dielectric substrate, commonly used for many high frequency digital and RF circuits, has signal traces on top and is backed by a conducting ground plane as shown in Fig. 1.

In a source-free region, the electric and magnetic fields can be obtained from the electric and magnetic Hertz vector potentials that satisfy Helmholtz equations. According to the boundary condition at $z=0$, it can be shown that only $\mathrm{TM}^{\mathrm{odd}}$ and $\mathrm{TE}^{\mathrm{even}}$ modes can be guided through the substrate. For the $\mathrm{TM}^{\mathrm{odd}}$ solutions, the field quantities in each of regions are given by [10]

$$\begin{aligned} E_{1x} &= -i\beta B\nu e^{-\nu x}e^{i\beta z} \\ E_{1z} &= -B\nu^2 e^{-\nu x}e^{i\beta z} \\ H_{1y} &= -iB\omega\varepsilon_1\nu e^{-\nu x}e^{i\beta z} \end{aligned} \tag{1}$$

and

$$\begin{aligned} E_{2x} &= i\beta A k_{2c}\cos(k_{2c}x)e^{i\beta z} \\ E_{2z} &= A k_{2c}^2\sin(k_{2c}x)e^{i\beta z} \\ H_{2y} &= iA\omega\varepsilon_2 k_{2c}\cos(k_{2c}x)e^{i\beta z} \end{aligned} \tag{2}$$

where the wavenumbers are given by

$$\begin{aligned} k_{2c}^2 &= k_2^2 - \beta^2 \\ \nu^2 &= \beta^2 - k_1^2 \end{aligned} \tag{3}$$

and A and B are some constants for each of regions.

From the continuity of the tangential electric and magnetic fields at $x=h$ and dispersion relations (3), the relations for k_{2c} and ν can be written as

$$\begin{aligned} \frac{\varepsilon_1}{\varepsilon_2}X\tan X &= Y \\ X^2+Y^2 &= \left(\omega h\sqrt{\mu_2\varepsilon_2-\mu_1\varepsilon_1}\right)^2 \end{aligned} \tag{4}$$

where $X=k_{2c}h$ and $Y=\nu h$.

The cutoff frequency for TM modes is defined as a frequency for which $\nu=0$, thus it is given by

$$f_{c_{\mathrm{TM}}} = \frac{m}{4h\sqrt{\mu_2\varepsilon_2-\mu_1\varepsilon_1}} \qquad \text{for } m=0,1,\ldots. \tag{5}$$

Here, it should be noted that $\mathrm{TM}_0^{\mathrm{odd}}$ has a zero cutoff frequency regardless of the substrate thickness, and only $\mathrm{TM}_0^{\mathrm{odd}}$ mode can be guided through a thin substrate. Therefore, $\mathrm{TM}_0^{\mathrm{odd}}$ mode mainly contributes to the mutual coupling observed in planar circuits.

To examine the characteristics of the dominant substrate mode, let us consider a relatively thick substrate near Bluetooth operating frequency. Solving (3) and (4) for $h=3.18$ mm, $\varepsilon_{1\mathrm{r}}=1$, $\varepsilon_{2\mathrm{r}}=2.2$, and $f=2.46$ GHz, the propagation constant and attenuation constant are obtained as $k_{2c}=56.252$, $\nu=4.599$, and $\beta=51.727$. The radio of the normal to horizontal components of the electric field at the interface in Region 1 (at $x=h^+$) is about -21 dB. Thus, the electromagnetic wave near the thin substrate can be approximated by a transverse electric and magnetic (TEM) wave. In fact

$$\frac{|E_z|}{|E_x|} = \frac{\sqrt{4\pi^2\left(\varepsilon_{2\mathrm{r}}-\varepsilon_{1\mathrm{r}}\right)\left(\frac{h}{\lambda}\right)^2-X^2}}{\sqrt{4\pi^2\varepsilon_{2\mathrm{r}}\left(\frac{h}{\lambda}\right)^2-X^2}} \qquad \text{at } x=h^+ \tag{6}$$

from which one can determine the region of validity of quasi-TEM approximation. Numerical simulation indicates that $|E_z|/|E_x| < -20$ dB can be maintained for substrates with $\varepsilon_{2\mathrm{r}} \le 10$ when $h/\lambda < 0.02$, and h/λ can be as high as 0.03 for $\varepsilon_{2\mathrm{r}} \le 2.2$. The characteristic impedance of this quasi-TEM wave is given by

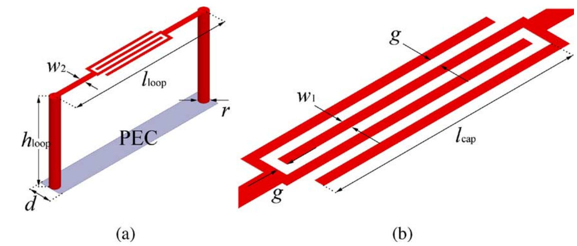

Fig. 2. Unit cell of the EBG isolator: (a) geometry of the EBG isolator; (b) geometry of the interdigital capacitor.

$$Z_{\mathrm{TM}} = \frac{|E_x|}{|H_y|} = \frac{\beta}{\omega\varepsilon_2} \tag{7}$$

which equates to $Z_{\mathrm{TM0}} = 171.8066\ \Omega$ at $f=2.46$ GHz.

III. Electromagnetic Band-Gap Isolator

The metamaterial-based EBG isolator is composed of single array of parallel LC resonant circuits that is magnetically coupled to the dominant substrate mode [9]. As can be seen in Fig. 2, the unit cell of the EBG isolator consists of vertical wires and horizontal conducting strips. The loop behaves like an inductor, and the interdigital metallic strips act as a series capacitor in the loop. For the quasi-TEM substrate mode, the horizontally polarized magnetic field is linked by the square loops of the EBG, which in turn induces electric currents on the vertical wires. This induced current generates a magnetic field in the opposite direction according to Lenz's law. When the unit cells are closely spaced to each other, the inductance of the loops is increased, and the periodic array acts like a solenoid. At resonant frequency, the periodic layer acts as a perfect magnetic conductor (PMC) plane and disturbs the propagation of the substrate mode.

Due to the mutual coupling between the adjacent loops, the self inductance of the square loop shown in Fig. 2 can be obtained from [6]

$$L_{\mathrm{S}} = \frac{\mu_r\mu_0 A_{\mathrm{loop}}}{d} \tag{8}$$

where $A_{\mathrm{loop}} = h_{\mathrm{loop}}\, l_{\mathrm{loop}}$ is the surface area of the loop, and d is the periodicity of unit cells.

As the induced current from the horizontal magnetic fields flows through the top conducting strips, it generates electric fields between the conducting strips. Since most of the electric fields between these strips are in the gap and perpendicular to the metallic edges, its capacitance can be computed from the capacitance per unit length of two thin coplanar strips given by [11]

$$C_{i,e} = \epsilon_{\mathrm{r}}\epsilon_0\frac{K(k_{i,e})}{K\left(\sqrt{1-{k_{i,e}}^2}\right)} \tag{9}$$

$$k_i = \sin\left(\frac{\pi}{2}\eta\right) \quad \text{and} \quad k_e = 2\frac{\sqrt{\eta}}{1+\eta} \tag{10}$$

TABLE I
DESIGNED PARAMETERS FOR THE EBG ISOLATOR

l_{loop}	l_{cap}	g	w_1	w_2
6.10 mm	2.34 mm	0.10 mm	0.10 mm	0.20 mm

h_{loop}	d	r	n
3.18 mm	0.81 mm	0.36 mm	4

where $\eta = w_1/(w_1+g)$ is the metallization ratio and $K(k)$ is the complete elliptic integral of first kind defined by

$$K(k) = \int_0^{\pi/2} \frac{d\phi}{\sqrt{1-k^2\sin^2\phi}}. \tag{11}$$

Since the individual capacitors between strips are connected in parallel, the total capacitance per unit length of interdigital capacitor is equal to

$$C = (n-3)\frac{C_i}{2} + 2\frac{C_iC_e}{C_i+C_e} \qquad \text{for } n>3 \tag{12}$$

where C_i is the capacitance between inner strips, C_e is between outer and inner strips, and n is the number of strips. Hence, the total capacitance of the proposed EBG isolator can be calculated easily from $C_{\text{S}} = Cl_{\text{cap}}$, where l_{cap} is the length of the strips. The designed parameters for operation at 2.46 GHz are summarized in Table I. The corresponding inductance and capacitance of the unit cell are thus found to be $L_{\text{S}} = 29.9237$ nH and $C_{\text{S}} = 0.1139$ pF, respectively.

IV. EQUIVALENT CIRCUIT MODEL FOR THE EBG ISOLATOR

As mentioned before, the substrate modes within a thin substrate can be approximated by a TEM plane wave. Also, the propagation of a TEM wave in a simple medium with material parameters ε and μ can be modeled in terms of an equivalent transmission-line with capacitance and inductance per unit length equal to ε and μ, respectively [12]. Hence, the propagation of the substrate mode within a thin substrate can also be represented using a transmission-line model as shown in Fig. 3. Due to the propagation symmetry along z-axis of the substrate, the Π transmission-line model is adopted. The inductance and capacitance per unit length of the transmission-line L_g and C_g are given by $\mu_{\text{r}}\mu_0$ and $\varepsilon_{\text{r}}\varepsilon_0$, respectively.

As the EBG isolator is linked to the substrate modes through the horizontal magnetic field, the inductance of the EBG structure can be modeled to have an inductive mutual coupling K_1 with the inductance of the equivalent transmission line as shown in Fig. 3(b). The induced electric currents on two vertical wires of the EBG flow in opposite directions, and therefore the equivalent inductor of the EBG isolator is divided into two equal inductances and connected to the ground plane of the transmission-line model. The mutual coupling between the vertical wires on the opposite sides is expressed by K_2. The mutual coupling between the equivalent transmission-line and the horizontal conducting strip of the EBG isolator can be described through the capacitive coupling C_{P2}. Furthermore, R_{S} and C_{P1} are employed to show the finite quality factor (Q) of the EBG isolator and the parasitic capacitance between the strips and ground plane, respectively.

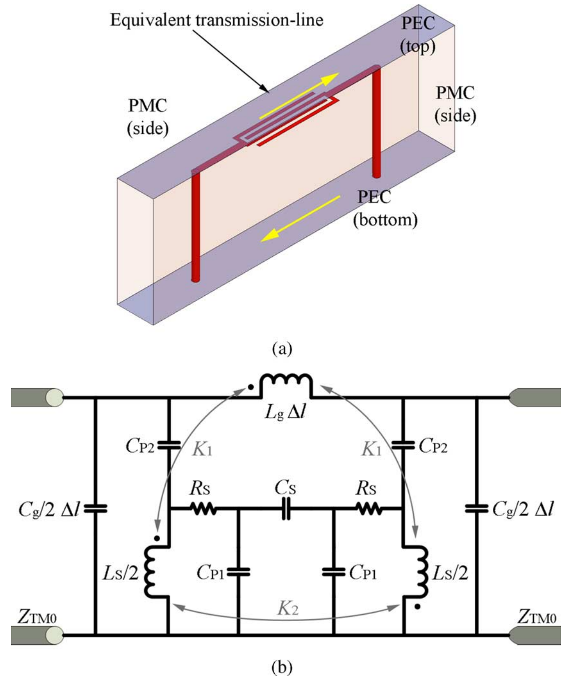

Fig. 3. Transmission-line model for the EBG isolator: (a) geometry of the equivalent transmission-line; (b) equivalent circuit model for the EBG isolator embedded substrate.

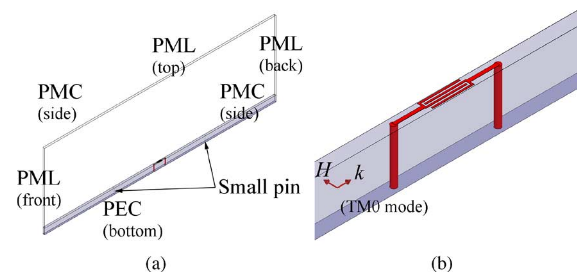

Fig. 4. (a) Boundary condition setup for full-wave simulation using finite element method solver. (b) Propagation of TM_0 mode within the substrate.

In order to verify the accuracy of the EBG isolator model, a commercial full-wave solver (Ansoft's HFSS ver. 12) is utilized. As shown in Fig. 4(a), PMC walls are assumed to enforce the periodic condition of the unit cells. To eliminate nonphysical reflections at the boundaries of the upper free space and the front and back sides, perfectly matched layers (PMLs) are assigned at these openings. Perfect electric conductor (PEC) is assigned at the bottom as an infinite ground plane. In addition, two small thin pins are employed to generate the substrate modes and measure the transmission coefficient through the EBG isolator. Since only TM_0 mode can be supported, the substrate mode is coupled to the EBG isolator as shown in Fig. 4(b).

In Section III, the inductance and the capacitance of the EBG isolator are analytically evaluated from (8) and (12). The equivalent transmission-line parameters are also analytically represented, and the set of values for the rest of circuit elements is derived from the result of full-wave simulations. A curve-fitting process using a high-frequency circuit simulator (Agilent's ADS 2008) is adopted to get the best fit between the circuit simulation and the full-wave response. It should be noted that a

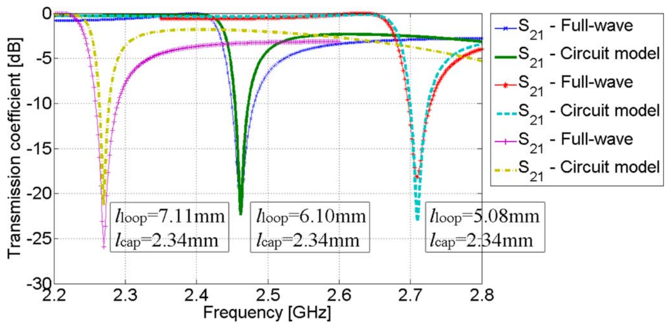

(a)

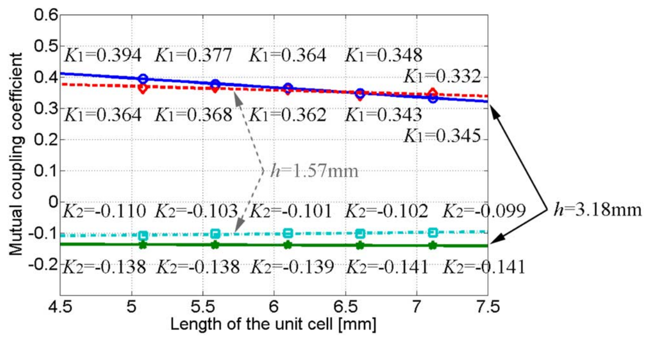

(b)

Fig. 5. (a) Comparison between full-wave and circuit simulation responses. (b) Simulated mutual coupling coefficients according to length of the unit cell.

TABLE II
EXTRACTED CIRCUIT ELEMENTS FOR THE PROPOSED EQUIVALENT CIRCUIT MODEL

L_S	C_S	R_S	C_{P1}	C_{P2}
29.9237 nH	0.1139 pF	0.65 Ω	10 fF	120 fF

Z_{TM0}	K_1	K_2	Δl
171.8066 Ω	0.364	-0.139	6.45 mm

normalized frequency response is obtained by dividing the frequency response (S_{21}) of the short vertical pins with and without the EBG. This approach is only valid to estimate the locations of the reflection zeros and poles of the EBG isolator. In addition, extremely dense meshes (very small tetrahedra) and very fine convergence in the finite element method (FEM) simulation are required to get accurate and stable results. The small tetrahedral meshes are required to model the gap capacitances and inductance of the loop accurately. The very fine convergence criteria is needed to get the resonant frequency of the high Q circuit correctly. The values of the circuit elements are summarized in Table II. As shown in Fig. 5(a), three different design parameter sets and corresponding capacitance/inductance with fixed circuit elements of R_S, C_{P1}, and C_{P2} are considered to estimate the mutual coupling coefficients K_1 and K_2. The proposed equivalent circuit model shows a good agreement with the full-wave responses including a reflection zero at 2.396 GHz and a bandstop response at 2.462 GHz.

Since the mutual coupling coefficients K_1 and K_2 account for the magnetic field linkage from the substrate mode and the EBG isolator, these values are dependent on the physical dimensions of the EBG isolator. Using the same curve-fitting process between the full-wave simulation and the proposed circuit model, the mutual coefficients are estimated according to the length of the EBG isolator as shown in Fig. 5(b). As the unit cell becomes longer, the inductive coupling between the substrate mode and the unit cell becomes weaker. However, the mutual coupling coefficient between the two vertical wires (K_2) shows little variations to the length of the unit cell within the small range ($\lambda_g/16 \sim \lambda_g/12$).

V. CONCLUSION

In this letter, the performance characteristics of single-layer 1-D periodic metamaterial-based EBG structures embedded in metal-backed substrates are described. It is shown that the dominant substrate mode for thin substrates can be approximated by a TEM wave inside and in the vicinity of the thin substrate. Given this TEM approximation, the magnetic coupling between the substrate mode and the EBG isolator is represented through a mutual inductive coupling and some capacitive couplings. An equivalent circuit model for the thin substrate embedding the EBG isolator is developed and analyzed. The circuit simulation response of the proposed equivalent circuit model shows a good agreement with the numerical full-wave solution. The proposed circuit model can be utilized to estimate the mutual coupling coefficients and to find the locations of the reflection zero and bandstop frequencies of the EBG isolator.

REFERENCES

[1] F. Yang and Y. Rahmat-Samii, “Microstrip antennas integrated with electromagnetic band-gap (EBG) structures: A low mutual coupling design for array applications,” *IEEE Trans. Antennas Propag.*, vol. 51, no. 10, pp. 2936–2946, Oct. 2003.

[2] K. Buell, H. Mosallaei, and K. Sarabandi, “Metamaterial insulator enabled superdirective array,” *IEEE Trans. Antennas Propag.*, vol. 55, no. 4, pp. 1074–1085, Apr. 2007.

[3] K. Payandehjoo and R. Abhari, “Employing EBG structures in multiantenna systems for improving isolation and diversity gain,” *IEEE Antennas Wireless Propag. Lett.*, vol. 8, pp. 1162–1165, 2009.

[4] S. Ghosh, T.-N. Tran, and T. Le-Ngoc, “A dual-layer EBG-based miniaturized patch multi-antenna structure,” in *Proc. IEEE Int. Symp. Antennas Propag.*, Jul. 2011, pp. 1828–1831.

[5] H. Mosallaei and K. Sarabandi, “A compact wide-band EBG structure utilizing embedded resonant circuits,” *IEEE Antennas Wireless Propag. Lett.*, vol. 4, pp. 5–8, 2005.

[6] H. Mosallaei and K. Sarabandi, “Design and modeling of patch antenna printed on magneto-dielectric embedded-circuit metasubstrate,” *IEEE Trans. Antennas Propag.*, vol. 55, no. 1, pp. 45–52, Jan. 2007.

[7] D. Sievenpiper, L. Zhang, R. Broas, N. Alexopolous, and E. Yablonovitch, “High-impedance electromagnetic surfaces with a forbidden frequency band,” *IEEE Trans. Microw. Theory Tech.*, vol. 47, no. 11, pp. 2059–2074, Nov. 1999.

[8] H. Mosallaei and K. Sarabandi, “Antenna miniaturization and bandwidth enhancement using a reactive impedance substrate,” *IEEE Trans. Antennas Propag.*, vol. 52, no. 9, pp. 2403–2414, Sep. 2004.

[9] K. Sarabandi and Y. J. Song, “Subwavelength radio repeater system utilizing miniaturized antennas and metamaterial channel isolator,” *IEEE Trans. Antennas Propag.*, vol. 59, no. 7, pp. 2683–2690, Jul. 2011.

[10] C. A. Balanis, *Antenna Theory*, 3rd ed. Hoboken, NJ: Wiley, 2005.

[11] R. Igreja and C. J. Dias, “Analytical evaluation of the interdigital electrodes capacitance for a multi-layered structure,” *Sensors Actuat. A, Phys.*, vol. 112, no. 2-3, pp. 291–301, 2004.

[12] R. Collin, *Foundations for Microwave Engineering*, 1st ed. New York: Wiley-IEEE Press, 2001.